Journal of Magnetic Resonance 192 (2008) 244–251

Contents lists available at ScienceDirect

Journal of Magnetic Resonance

journal homepage: www.elsevier.com/locate/jmr

MAS NMR spectra of quadrupolar nuclei in disordered solids: The Czjzek model

Jean-Baptiste d'Espinose de Lacaillerie [a,*], Christian Fretigny [a], Dominique Massiot [b]

[a] Physico-chimie des Polymères et des Milieux Dispersés, UMR 7615 CNRS UPMC, ESPCI ParisTech, 10 rue Vauquelin, 75005 Paris, France
[b] Centre de Recherches sur les Matériaux à Hautes Températures, UPR 4212 CNRS, 1D avenue de la Recherche Scientifique, 45071 Orléans Cedex 2, France

ARTICLE INFO

Article history:
Received 17 December 2007
Revised 28 February 2008
Available online 6 March 2008

Keywords:
Solid-state NMR
Quadrupolar nuclei
Amorphous materials
Glass
Gel
Aluminum-27
Lineshape
Electrical field gradient
Disorder

ABSTRACT

Structural disorder at the scale of two to three atomic positions around the probe nucleus results in variations of the EFG and thus in a distribution of the quadrupolar interaction. This distribution is at the origin of the lineshape tailing toward high fields which is often observed in the MAS NMR spectra of quadrupolar nuclei in disordered solids. The Czjzek model provides an analytical expression for the joint distribution of the NMR quadrupolar parameters υ_Q and η from which a lineshape can be predicted. This model is derived from the Central Limit Theorem and the statistical isotropy inherent to disorder. It is thus applicable to a wide range of materials as we have illustrated for ^{27}Al spectra on selected examples of glasses (slag), spinels (alumina), and hydrates (cement aluminum hydrates). In particular, when relevant, the use of the Czjzek model allows a quantitative decomposition of the spectra and an accurate extraction of the second moment of the quadrupolar product. In this respect, it is important to realize that only rotational invariants such as the quadrupolar product can make sense to describe the quadrupolar interaction in disordered solids.

1. Introduction

Solid-state nuclear magnetic resonance (NMR) of quadrupolar nuclei has recently turned into a precise tool for structural analysis. In many cases, the quadrupolar interaction can be measured with good accuracy thanks to instrumental advances such as strong radio frequency and static fields. At the same time, density functional theory based computational methods can relate *ab initio* the electrical field gradient (EFG), and in turn the quadrupolar interaction, to structural data. In the best case scenario, one can thus calculate the powder-averaged NMR spectrum for a proposed structure and confront it with the experimental data. This situation is very satisfactory and leads to solid conclusions as no empiricism is at stake [1]. However, when studying materials which are not perfectly ordered, the situation can be appreciably more complex. The NMR response from an ensemble of resonating probe nuclei is the superposition of the responses of all the possible environments for the nuclei in the sample. So, if statistical disorder is significant within the volume element contributing to the EFG at the nucleus, the NMR spectrum results from a distribution of the quadrupolar interaction parameters (which superimposes itself onto the usual powder average). *In toto*, the powder NMR spectrum is the summed contributions from all the nuclei experiencing different quadrupolar interactions in randomly oriented crystallites. The quadrupolar interactions are distributed in a manner which reflects the distribution of the EFG, which in turn is the expression of structural disorder at the relevant scale. To be able to provide a structural interpretation of the NMR spectra of disordered materials, it is thus necessary to formulate a probability density function (PDF) to describe the distribution of the parameters defining the strength (υ_Q) and shape (η) of the quadrupolar interaction tensor. This not so trivial problem of applied statistics (going from spatial, or electronic, disorder to a distribution of the EFG and finally to a distribution of quadrupolar parameters) was solved at the beginning of the eighties by Czjzek within the context of Mossbauer spectroscopy [2] and later successfully applied to Electron Spin Resonance and Perturbed Angular Correlations technique in glasses [3–6] and alloys [7,8]. It has been, however, only recently that several authors have advocated the use of the Czjzek model for the analysis of the magic angle spinning (MAS) NMR spectra of disordered materials, glasses [9–12] and spinel-type solids [13]. In particular, it was very recently implemented in a free and widely distributed NMR simulation software [14].

In this article, considering the growing importance of the Czjzek lineshape within the NMR community, we will attempt to clarify the arguments underlying the derivation and use of the Czjzek model. For that purpose, we will first review and evaluate existing approaches to the issue of the distribution of quadrupolar parameters in NMR. Then we will present in detail the joint probability density function (PDF) of the quadrupolar parameters derived by Czjzek, explaining its physical significance and practical

* Corresponding author. Fax: +33 1 40 79 47 44.
E-mail address: Jean-Baptiste.dEspinose@espci.fr (J.-B. d'Espinose de Lacaillerie).

1090-7807/$ - see front matter © 2008 Elsevier Inc. All rights reserved.
doi:10.1016/j.jmr.2008.03.001

consequences for NMR. In particular, we will assess its experimental validity on non-glassy disordered materials. Finally, we will illustrate on a cement sample the potential of the Czjzek model for a quantitative analysis of the spectra of multiphasic ill-crystallized samples.

2. Distribution of quadrupolar parameters

It is an experimental fact that structural disorder results in a distribution of quadrupolar parameters and non-zero quadrupolar coupling even for nuclei in environments of high local symmetry. Hence, for example, the occurrence of a measurable quadrupolar effect on the ^{87}Sr resonance in $SrCl_2$ [15]. This is the expression of the non-locality of the quadrupolar interaction: Considering solely the orbitals centered at the nucleus is not sufficient for an accurate determination of the EFG. Although the EFG, that is the non-spherical distribution of charges around the nucleus, is largely determined by valence electrons and first-shell chemical bonding, the "exterior", or "crystal", orbitals have also to be taken into account. Structural disorder at the scale of two to three atomic positions around the probe nucleus results in variations of the EFG and thus in a distribution of the quadrupolar interaction. Due to limited computational time, the usual model clusters employed to calculate *ab initio* the EFG extend rarely beyond the third coordination sphere of the probe nucleus. Nevertheless, crystalline distortions well beyond that range have indeed been predicted to have a significant cumulative effect on the EFG [16–18].

Regarding the chemical shift, structural imperfections are commonly assumed empirically to result in a Gaussian broadening (although this assumption might not be strictly and generally founded [19,20]). By analogy, the same approach could be taken to account for the effect of disorder on the quadrupolar interaction. However, a Gaussian broadening of the quadrupolar lineshape does not reproduce the asymmetric quadrupolar lineshape often observed in disordered materials (see Fig. 1 for example). The origin of a lineshape tailing toward high fields is understandable, considering that to second-order, the quadrupolar interaction results in a high field shift and therefore in an unidirectional broadening of the powder spectrum proportional to the strength of the interaction. If this strength is distributed, the resulting lineshape necessarily tails in that direction. The Czjzek model allows us to go beyond this pictorial representation and to provide an analytical expression for the lineshape.

2.1. NMR resonance of a quadrupolar nucleus

Let us first formalize the problem. The quadrupolar interaction Hamiltonian expresses the coupling of a nucleus of spin I and electric quadrupole moment Q with an electric field gradient tensor V (whose elements are the partial derivatives of the potential) through

$$H_Q = \left(\frac{eQ}{2I(2I-1)h}\right)\hat{I}\cdot V\cdot\hat{I} \tag{1}$$

where e is the elementary charge and h the Plank's constant. Any physical manifestation of this coupling will thus depend on the nine V_{ik} elements of the 3×3 V matrix. These elements originate from the additive contribution of a number of structural elements which are each described by a set of independent parameters. Thus, for example, the independent parameters could be, but are not restricted to, the coordinates of all the atoms needed to describe the local structure needed to compute the EFG. The number of structural variables involved is thus potentially very large. Nevertheless, the EFG being constrained by the Laplace equation imposing symmetry and vanishing trace, only five independent

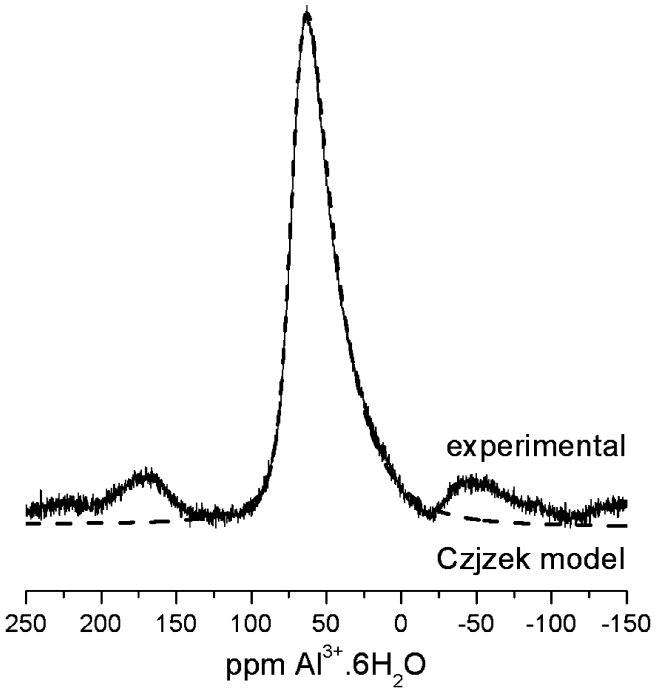

Fig. 1. One-pulse ^{27}Al MAS NMR spectrum of a slag sample. The Czjzek model (dashed line) is well adapted to the description of the experimental spectrum (noisy solid line). The spectrum is interpreted as resulting from a single tetrahedral environment distributed according to $\delta_{iso} = 72.7$ ppm and $\sigma = 467$ kHz. The latter value corresponds to, see Eq. (7), a root mean square quadrupolar product $\sqrt{\langle C_{Q\eta}^2\rangle}$ of 6.96 MHz.

variables are actually needed to describe the nine V_{ik} terms of the EFG matrix. Several sets of variables can be chosen, but it is customary in NMR to describe the quadrupolar interaction through the so-called quadrupolar parameters

$$\Omega_Q = (\nu_Q,\quad \eta,\quad \alpha,\quad \beta,\quad \gamma)$$

defined relatively to the diagonalized EFG through

$$\nu_Q = \frac{3eQ}{2I(2I-1)h}V_{ZZ}\quad\text{and}\quad \eta = \frac{V_{XX}-V_{YY}}{V_{ZZ}} \tag{2}$$

where $|V_{XX}|\leqslant|V_{YY}|\leqslant|V_{ZZ}|$ are the three sorted eigenvalues of the EFG (α, β, and γ being the Euler angles defining the corresponding principal axis system).

Finally, from the set of five quadrupolar parameters Ω_Q, the effect of the quadrupolar interaction on the MAS NMR spectra can be computed. For example, the frequency of the central transition associated with the quadrupolar interaction treated as a second-order perturbation of the Zeeman is given to by

$$\nu(\Omega_Q) = \left(\frac{\nu_Q^2}{\nu_0}\left[I(I+1)-\frac{3}{4}\right]\right)\left(-\frac{1}{30}\left[1+\frac{\eta^2}{3}\right]+\frac{1}{360}f_1(\alpha,\beta)\right) \tag{3}$$

where $f_1(\alpha,\beta)$ is given in Ref. [21] and ν_0 is the Larmor frequency. Note that f_1 is independent from γ. The physical response for a single nucleus experiencing a quadrupolar interaction of parameters Ω_Q is thus formally represented by a response function which is simply a Dirac delta function (neglecting any residual linewidth)

$$s(\nu;\Omega_Q)\sim\delta[\nu-\nu(\Omega_Q)]$$

For an ensemble of nuclei experiencing different quadrupolar interactions, the spectrum is the sum of all the individual responses of each nucleus or, equivalently, the sum of each possible response weighted by the number of nuclei experiencing the corre-

sponding quadrupolar interaction (eventually further weighted by the radio frequency excitation profile but we will not consider this in our discussion)

$$S(\nu) \sim \sum_{n}^{\text{all nuclei}} \delta_n[\nu - \nu(\Omega_{Qn})] = \sum_{i}^{\text{all different environments}} N_i(\Omega_{Qi})\delta_i[\nu - \nu(\Omega_{Qi})]$$

In a disordered sample, due to the residual linewidth and to the large number of the randomly distributed environments, the quadrupolar parameters Ω_Q can be considered random variables and the PDF of Ω_Q substitutes to $N(\Omega_Q)$. We can thus write the formal expression of the full spectrum as the average of the response function whose arguments are the quadrupolar random variables Ω_Q [22]

$$S(\nu) \sim \int p_{\Omega_Q}(\Omega_Q)\delta[\nu - \nu(\Omega_Q)]\mathrm{d}\Omega_Q$$

For the MAS NMR spectrum of a randomly oriented powder, considering that there is no correlation between the orientation of the EFG and its eigenvalues,

$$p_{\Omega_Q}(\Omega_Q) = p_{\text{angles}}(\alpha,\beta,\gamma)p_Q(\nu_Q,\eta) = \frac{1}{8\pi^2}p_Q(\nu_Q,\eta)$$

where $1/8\pi^2$ is the constant PDF of the angles random variables and p_Q the PDF of the remaining random variables (ν_Q, η). One thus gets

$$S(\nu) \sim \int_{-\infty}^{+\infty}\int_0^1 p_Q(\nu_Q,\eta)\left\{\int_0^{2\pi}\int_0^{2\pi}\int_0^{\pi} \times \frac{1}{8\pi^2}\delta[\nu - \nu(\Omega_Q)]\sin\beta\,\mathrm{d}\beta\,\mathrm{d}\alpha\,\mathrm{d}\gamma\right\}\mathrm{d}\eta\,\mathrm{d}\nu_Q \quad (4)$$

Thus the spectrum results from two successive summations. The first summation, over all possible orientations of the EFG, is the well-known powder average for given values of (ν_Q,η). There is no analytical solution to the corresponding integral, and the powder lineshape is commonly generated by numerical sampling of the angles [14]. The second summation is the weighted average of the powder lineshapes over all possible (ν_Q,η). Finally, $\nu(\Omega_Q)$ being independent from γ, the Eq. (4) can be simplified as

$$S(\nu) \sim \int_{-\infty}^{+\infty}\int_0^1 p_Q(\nu_Q,\eta) \times \left\{\frac{1}{4\pi}\int_0^{2\pi}\int_0^{\pi}\delta[\nu - \nu(\Omega_Q)]\sin\beta\,\mathrm{d}\beta\,\mathrm{d}\alpha\right\}\mathrm{d}\eta\,\mathrm{d}\nu_Q \quad (5)$$

This formalism leads us to the necessary conclusion, already stated in the introduction, that the issue of modeling and understanding the quadrupolar spectrum of disordered materials is reduced to the one of finding the joint PDF of the quadrupolar parameters $p_Q(\nu_Q,\eta)$. Although it can be performed numerically by numerical molecular dynamics simulations [23], the random character of the structures under consideration opens, as we will see, the possibility to derive an analytical expression of the PDF through the applied statistics formalism.

2.2. The Czjzek model

Two tempting simplifications could be implemented. First, one could distribute the quadrupolar parameters υ_Q and η with independent normal PDFs. And second, their distributions could be taken as Gaussians. Albeit easy to implement, these approaches are unfortunately not physically founded. In the first place, there is no justification for the choice of independently distributing υ_Q and η. Indeed, the electronic structure around the nucleus is a reflexion of its bonding environment, and it is hard to conceive a situation where a distortion of the electronic structure would impact an eigenvalue along one principal axis and not the eigenvalues along the ones in the perpendicular plane. In other words, the modification of υ_Q must be associated with a modification of η. Those two variables are not independent. In the second place, the distributions cannot be considered Gaussians. Indeed, the Central Limit Theorem, which founds the use of a normal distribution does not apply to the quadrupolar parameters. The reason is that the structural parameters do not contribute in an additive manner to the quadrupolar parameters since they derive from eigenvalues.

On the other hand, the structural parameters do have an additive contribution to the tensor elements of the EFG. The Central Limit Theorem thus applies to the elements of the EFG, and they can consequently be predicted to tend toward a normal distribution. Indeed, Jaeger et al. [24,25], following Meinhold et al. [26], have numerically constructed discrete distributions of υ_Q from normal distributions of the EFG tensor elements with the constraints necessary to impose symmetry and tracelessness on the EFG. The value of η is fixed but considered as an adjustable parameter. Although this numerical approach still treats disjointly η and υ_Q, this drawback is tempered by the fact that the resulting lineshape does not depend strongly on η. Others have also followed the approach of Meinhold but, from the distribution of the EFG, they produced a numerical distribution of pairs of η and υ_Q [27]. These two methods are physically sound but do not provide an analytical expression for the PDFs of η and υ_Q, and the discussion of the structural information content of the NMR spectrum is consequently limited. For this reason, Hoatson [28] has advocated for the use of Gaussian distributions of η and υ_Q. The rational is that, although not physically justified, they do produce empirical lineshapes very similar to the experimental ones while, since the mean and variance of the traditional quadrupolar parameters η and υ_Q are directly adjusted, the results are more conveniently interpreted in terms of structural disorder. As we shall see, this argument is debatable as the Czjzek model precisely calls into question the very existence of η and υ_Q as pertinent physical descriptor of disordered materials.

Using random variable theory, Czjzek proposes the following joint PDF (see the annex for the essential steps of its derivation)

$$p_Q(\nu_Q,\eta) = \frac{1}{\sqrt{2\pi}\sigma^5}\nu_Q^4\eta\left(1-\frac{\eta^2}{9}\right)\exp\left[-\frac{\nu_Q^2\left(1+\frac{\eta^2}{3}\right)}{2\sigma^2}\right] \quad (6)$$

where the parameter σ is the width of the distribution of the elements of EFG.

2.3. Consequences of the Czjzek model

An essential feature of this expression is that the PDF depends on a single parameter σ which will determine the shape of the distribution and ipso-facto of the MAS NMR line. It relates to the second moment of the quadrupolar product (proportional to the norm of the EFG) through

$$\left\langle C_{Q\eta}^2\right\rangle = \left(\frac{2}{3}I(2I-1)\right)^2\left\langle \nu_Q^2(1+\eta^2/3)\right\rangle = \left(\frac{2}{3}I(2I-1)\right)^2 5\sigma^2 \quad (7)$$

In order to assess the applicability of this PDF for the purpose of the solid-state NMR of quadrupolar nuclei, we recall below the assumptions which underlie its derivation:

(i) the structural elements contribute additively to the EFG
(ii) the sets of random variables defining the structural elements constitute independent random variables
(iii) the number of structural elements contributing to the EFG is "sufficiently" large
(iv) the ensemble of structural elements responsible for the EFG constitute a statistically isotropic solid.

The first three points insure that by virtue of the Central Limit Theorem, the EFG tensor elements each approach a multivariate normal distribution, while the fourth point insures that the EFG tensor elements are identically distributed. Point (i) does not call for any restriction but points (ii) and (iv) restrict it to matter not ordered at a scale exceeding the range of the quadrupolar interaction (or, incidentally, at a scale orders of magnitude larger than the quadrupolar range [29]). However, this does not imply any restriction in terms of local order. Obviously, if statistical isotropy meant an isotropic environment for the nucleus, the EFG would be nonexistent, and there would be no quadrupolar interaction in disordered materials. The most restrictive point actually appears to be point (iii) which implies a sufficient number of contributing neighbors. This means that, for a given number of contributing coordination shells, a "large enough" coordination number is required. How "large" is "enough" for the PDF of the EFG tensor elements to be approximated by a normal distribution is difficult to rationalize. Our experience is that it requires a coordination of four or more for the probe nuclei. This unfortunately excludes *de facto* the important case of ^{17}O NMR in oxide glasses.

3. Experimental validation and use of the Czjzek model

Glassy materials are subject of choice for applying the Czjzek model. In particular, one of us was able to refine the local structure of calcium aluminosilicate glasses by modeling their ^{27}Al NMR spectra using the Czjzek approach [30]. As a further example, we present here the spectrum of a quenched molten slag (the low-density melt residue obtained during the production of pig iron). This slag is actually a calcium aluminosilicate glass with a ratio $R = CaO/Al_2O_3$ of 4. It can thus be considered as a percalcic glass with intermediate silica content (30% SiO_2). Its ^{27}Al MAS NMR powder spectrum is a near perfect match for the Czjzek model with an isotropic chemical shift of 72.7 ppm and an adjustable parameter σ of 467 kHz (Fig. 1). The corresponding value for the root mean square quadrupolar product (Eq. (7)) of 6.96 MHz is very close to the average quadrupolar product measured by MQMAS on synthetic percalcic aluminosilicates [30], and the chemical shift is exactly what could be predicted from the known linear dependency of the chemical shift of tetrahedral aluminum on the silica content in aluminosilicate glasses [11]. Furthermore, the fact that only one Czjzek lineshape was needed to model the spectrum reveals that only one type of coordination was present despite the moderate silica content and the high level of impurities (nearly 20% by weight). In particular, thanks to the Czjzek model, unresolved five- and sixfold coordination can be excluded with a high level of confidence even though the resonance significantly tails toward chemical shift ranges normally typical of these coordinations. In summary, the modeling of the resonance by way of the Czjzek PDF allows for a precise discussion of the structural information content of the NMR spectra of glasses.

Apart from glasses, published applications of the Czjzek model to date relate to the quantification of sites in defective spinel structures [31]. Such materials constitute a good test for whether or not its application must be restricted to truly amorphous or glassy materials. For this reason, we now present and discuss the ^{27}Al one-pulse MAS NMR spectrum of γ-alumina. Although it presents only broad X-ray diffraction patterns (not shown), this alumina polymorph is not amorphous in the sense that it has a definite long-range defective spinel structure where short-range order consists of octahedral and tetrahedral elementary units [32]. Actually, the occurrence of five-coordinated aluminum can be taken as a measure of medium-range disorder [33]. In this respect, the spectrum of Fig. 2 shows no occurrence of a resonance around 30 ppm indicative of the pentacoordination of aluminum,

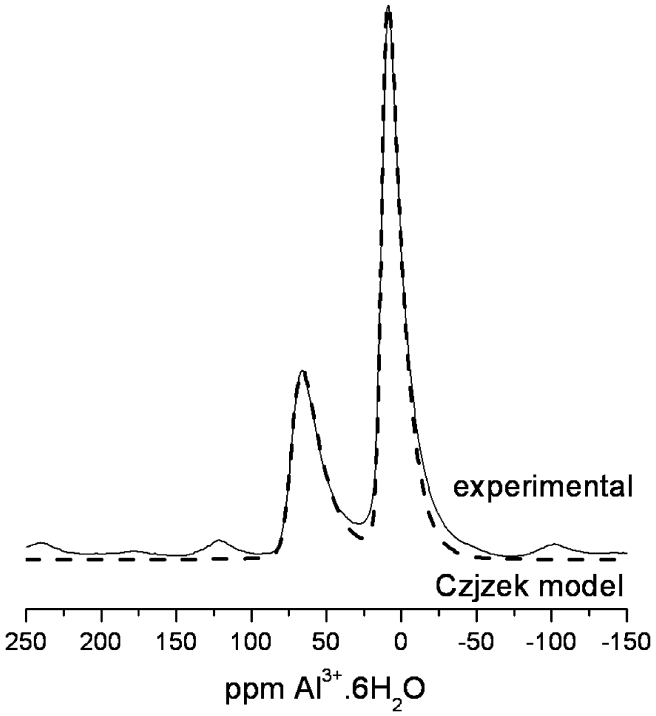

Fig. 2. ^{27}Al one-pulse MAS NMR spectrum of γ-alumina. Although the fit (dashed line) is not as perfect as in the glass sample (Fig. 1), the model is still satisfactory. The spectrum is interpreted as the sum of two Czjzek contributions in a 2:1 ratio corresponding to the ideal ratio of tetrahedral (δ_{iso} = 73.8 ppm and σ = 405 kHz) to octahedral aluminum (δ_{iso} = 13.8 ppm and σ = 340 kHz) in the spinel structure.

and our sample can thus be considered well-structured. The structural formula (corresponding to a sub-cell of 3/4 of the unit cell) can be written as $(\square)_2(Al^{VI})_{12-x}(Al^{IV})_{6-y}O_{24}$ where $x + y = 2$ is the total number of cationic vacancies.These vacancies are distributed between the octahedral and tetrahedral cationic sites. The total number of possible combinations per sub-cell is 153. From DFT calculations, it has been shown that all combinations are very close in energy and thus it is likely that a significant number of them coexist at room temperature [34]. As a consequence, despite the structured atomic arrangement, the distribution of vacancies results in a large number of possible environments for each aluminum nucleus. This explains why the spectral singularities of the quadrupolar lineshapes have disappeared from the MAS NMR spectrum (Fig. 2). Here again, it could be successfully decomposed in lineshapes following the Czjzek model. The model of Czjzek thus appeared robust and applicable to a wide range of disordered materials, well beyond the case of ideal glasses.

4. Practical significance of the Czjzek model

First and foremost, the practical motivation for the use of Czjzek model in the context of MAS NMR of quadrupolar nuclei is to provide a quadrupolar lineshape for disordered materials so as to be able to decompose quantitatively and accurately their spectra. After validating this approach on known samples, we now will show on a complex multi-phase sample how, from a simple one-pulse experiment, it can improve the quantitative analysis of the NMR spectrum. This is exemplified in the case of the speciation and quantification of the sulfo-aluminate hydrates in cement mineralogical assemblage.

Hydration of the calcium aluminates in anhydrous cement leads to a mixture of trisulfo-aluminate, of monosulfo-aluminate and of

an ill-defined amorphous aluminum hydrate. The need to identify and quantify these species is driven by the fact that the mechanical stability of cement depends in part from the stability of this mineral assemblage when exposed to external sources of sulfate ions such as the ones found in the soil or in sea water. Such a quantitative analysis of aluminum hydrates in cement is currently limited and possible in part only through a Rietveld analysis of low angles XRD patterns [35]. So far, MAS NMR was considered to fail for that purpose precisely because of the quadrupolar character of ^{27}Al and of the disordered nature of the sample leading to broad overlapping resonances which could not be separated due to their unknown lineshapes. The use of Czjzek model has solved this issue and allowed for an accurate quantification of these phases as seen in Fig. 3 and Table 1. The isotropic chemical shifts are in line with the literature for the considered phases. In trisulfo-aluminate, aluminum occurs in a highly symmetrical sixfold coordination [36]. Consequently, it experiences no EFG and no quadrupolar effects and the corresponding lineshape is a simple Lorentzian. Monosulfo-aluminate on the other hand is poorly crystallized and is thus distributed according to the Czjzek model. TAH being a totally XRD amorphous hydrate of unknown structure [37] is largely broadened according to Czjzek's PDF of quadrupolar parameters with a value of σ double the one of the more structured monosulfo-aluminate. Actually, it might be interesting to discuss the small but significant departure of the experimental lineshape at high field from the Czjzek model (lower trace of Fig. 3). This deviation in itself carried information obviously unreachable without using the Czjzek model. It indicates either the existence of a fourth species or the fact that the third aluminum hydrate is not truly amorphous (to a smaller extent, the same observation could have been made for the octahedral resonance in the spectrum of γ-alumina). In this respect, Le Caër has discussed numerically how a departure from hypothesis (ii) (namely a remaining level of correlations between the structural elements) affects the Czjzek lineshape [38]. He thus defines the so-called degenerate model by empirically modifying the exponent of σ in Eq. (6). Although the degenerate model, by introducing an empirical adjustable parameter (the exponent), might allow a better fit of the lineshape, this result would be obtained at the expense of the physical meaning of the PDF. Again, at this stage, it is safer to simply conclude that the third aluminum hydrate is not truly amorphous.

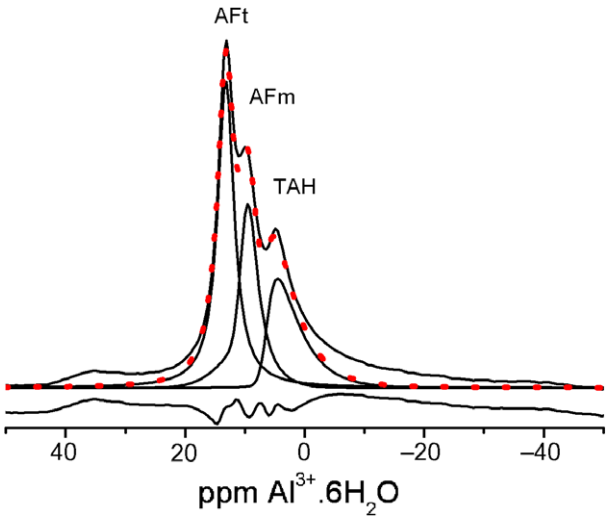

Fig. 3. Octahedral frequency range of the one-pulse ^{27}Al MAS NMR spectrum of a hydrated cement paste. The solid lines are the traces of the experimental spectrum and of the fitted models of trisulfo-aluminate (AFt or Ettringite), monosulfo-aluminate (AFm or sulfate form of hydrocalumite) and the "third aluminum hydrate" (TAH). The dotted line is the total modeled spectrum. The lower trace represents the difference between the experimental and modeled spectra. No attempts are made to model the pentahedral frequency range around 30 ppm. Model parameters are given in Table 1.

Table 1
Model parameters used to fit the ^{27}Al MAS NMR spectrum of the hydrated cement paste (Fig. 3)

$\delta_{CS}^{(iso)} \pm 0.1$ ppm	Model	$\sigma \pm 10$ kHz	$\sqrt{\langle C_{Q\eta}^2 \rangle} \pm 0.15$ MHz	Amplitude ±2 (%)	
13.2 ppm	Lorentz			41	AFt
10.3 ppm	Czjzek	118 kHz	1.76 MHz	30	AFm
6.5 ppm	Czjzek	224 kHz	3.34 MHz	18	TAH
≈−10 ppm				11	Unassigned

5. Discussion

We have seen in the two preceding sections the strong practical advantages of resorting to the Czjzek model. First, by comparing the experimental spectrum to the Czjzek model, we can test if the characteristics of the material correspond to the hypothesis of the model, noticeably with respect to statistical isotropy and persistent positional correlations within the solid. Second, once the model is validated for the solid under consideration, we can now decompose overlapping resonance and thus accurately quantify crowded spectra. Although this is probably the main interest of the Czjzek model, it is also interesting to note that it constitutes a good support for discussing the information content of the MAS NMR spectra of disordered solids.

In disordered solids, we can of course always obtain from a NMR measurement the marginal distribution of the quadrupolar parameters. Within the Czjzek model, this could be accomplished by fitting the experimental MAS NMR lineshape to a value of the parameter σ from which, for instance, the average value of η (Eq. (14) of the annexe) and the root mean square of υ_Q (Eq. (15) of the annex) could be calculated. However, the use of the Czjzek model showed that an analysis of the EFG in disordered solids in those terms would not be necessarily the most relevant. This is particularly clear for the averaged value of η which is constant in the Czjzek model. Actually, its marginal distribution is not even parameterized and thus evidently carries no structural information besides the fact that the material obeys the prerequisite of the Czjzek model. In conclusion, it might be best for disordered solids to abandon a description of the NMR manifestation of the EFG in terms of η and υ_Q.

In disordered solids, statistical isotropy results in a drastic reduction of the independent variables. A direct consequence is the fact that the distributions of η and υ_Q are necessarily jointed. Furthermore, only rotational invariants of the EFG could make physical sense to describe the structure. In this respect, the Czjzek model, allowing for the derivation of an analytical expression for this joint PDF, provides a direct way to characterize a rotational invariant, namely the norm of the EFG. Indeed, from Eq. (7), we realize that the fitting parameter σ stands physically, to a proportionality constant, for the root of the second moment of the quadrupolar product, which is itself proportional to the norm of the EFG. Lineshape fitting of the resonance by way of the PDF resulting from the Czjzek model thus provides a simple and convenient mean to extract the second moment of the quadrupolar product from the NMR spectra.

Even without the help of the Czjzek model, it has long been realized that only the second moment of the quadrupolar product could be extracted from the shapeless resonance of quadrupolar nuclei in disordered materials. For that purpose, the well-known relationship between the mean square quadrupolar product and the center of gravity of the resonance of quadrupolar nuclei was used [39]

$$\nu_{cg} = -\frac{3}{40}\frac{\left\langle C_{Q\eta}^2 \right\rangle}{(I(2I-1))^2\nu_0}\left[I(I+1)-\frac{3}{4}\right] \quad (8)$$

This approach is more general since it is does not rely on the choice of a PDF to calculate the mean square quadrupolar product but simply estimates it from the first moment of the resonance line. However, it suffers from two experimental drawbacks. First, it relies on an integrated measurement of the resonance which makes it dependent on the experimental frequency cut-off values and on the quality of the baseline. Second, making no assumption about the PDF, it does not provide a model lineshape and consequently cannot separate the contributions of overlapping resonances. Since it necessitates the integration of the full lineshape, it is essentially limited to fully resolved resonances.

On the contrary, the procedure derived from the Czjzek model does not suffer from these limitations. Being based on a full lineshape analysis, all data points must fit the model, allowing for a greater degree of confidence, a sorting out of baseline distortions, and an extrapolation to decompose overlapping resonances. Along the same line, the fact that Czjzek modeling leads to a higher estimate of the average quadrupolar coupling constant than MQMAS has been noted in a recent study of alumosilicate melts [40]. This was attributed to the difficulty to detect the broad contributions associated with strong quadrupolar couplings and, thus, to a biased determination of the position of the center of gravity of the MQ resonance in the direct and indirect dimensions. We can complete this statement by emphasizing that even when the high frequency end of the spectrum is lost in the noise, Czjzek modeling permits, all the same, to extract the root mean square quadrupolar product from the spectrum simply by fitting the sharp apparent part of the resonance (and making use of Eq. (7)).

6. Conclusion

In summary, the Czjzek model, being based solely on the Central Limit Theorem and on statistical isotropy, appears to be applicable to the NMR spectra of a wide range of disordered materials. It remains, however, limited to quadrupolar nuclei with a coordination at least equal to four. Its interest lies in the fact that providing a lineshape parametrized by the second moment of the quadrupolar product, it allows a better estimate of the root mean square quadrupolar product than other existing methods based on the determination of the center of gravity of one-pulse or multiple-coherence (MQMAS) resonances. Furthermore, the knowledge of the lineshape allows for a safe quantitative decomposition of overlapping resonances and a test of their disordered character.

7. Experimental

7.1. MAS NMR

Magic angle spinning nuclear magnetic resonance (MAS NMR) experiments were performed in 4 mm zirconia rotors on Bruker ASX spectrometers at 7.05 T, 11.7 T (ESPCI, Paris) and Bruker DSX spectrometers at 19.6 T (NHMFL, Tallahassee). ^{27}Al one-pulse experiments were performed spinning at 14 kHz with a selective pulse ($<\pi/6$) duration of 0.5 μs, recycle time 1 s and between 300 and 200,000 acquisitions depending on the samples. According to the static fields, the rf fields were 78.19, 130.31 and 216.13 MHz at 7.02, 11.7 and 19.6 T, respectively.

7.2. Modeling

The experimental spectra are fitted to models using the free DMfit software. The central transition is modeled by the Czjzek model. When spinning side bands are present, the first satellite transition and its first side bands are modeled using Lorentzian lineshapes. The isotropic chemical shift is constrained to be identical for the central and satellite transitions.

7.3. Materials

Blast furnace slag sample (courtesy of Dr. Albert, Lafarge) from Fos (France) is a glassy by-product of the steel industry. Typical composition is 40% CaO, 30% SiO_2, 10% Al_2O_3, and the rest being MgO, FeO, and sulfides. γ-Al_2O_3 is obtained by calcination 4 h at 773 K of boehmite supplied by Condea. Cement samples are class G Portland cement hydrated with a water/cement ratio of 0.4 and cured 30 days under room conditions.

Appendix A. Derivation of the Czjzek model

We will here briefly summarize the fundamental steps of the derivation of the Czjzek model. A more thorough explanation can be found in Ref. [38].

A.1. Disorder and distribution of quadrupolar parameters

We start from Eq. (5) which is justified in the text

$$S(\nu) \sim \int_{-\infty}^{+\infty}\int_0^1 p_Q(\nu_Q,\eta)\left\{\frac{1}{4\pi}\int_0^{2\pi}\int_0^{\pi}\delta[\nu-\nu(\Omega_Q)]\ \sin\beta \mathrm{d}\beta\mathrm{d}\alpha\right\}\mathrm{d}\eta\mathrm{d}\nu_Q$$

with $\nu(\Omega_{Q_s})$ given by Eq. (3).

For materials disordered at a lower scale than the quadrupolar range, it is thus evident that a lineshape analysis requires knowledge of the joint PDF $p_Q(\nu_Q,\eta)$ which in turn derives in principle from the distribution of the structural parameters. The latter distribution can vary and might actually be unknown; but, as we will see later, an important point is that in many physical systems allowing for a large number of degree of freedom, the structural parameters can be assumed to constitute independent random variables of finite variance. The validity of this assumption is essential to any statistical treatment of the quadrupolar interaction as it justifies the use of the Central Limit Theorem.

The Czjzek model's first step: Central Limit Theorem and choice of a representation of the EFG

As pointed out by Le Caër [38], the additivity of the physical contributions holds for the EFG tensor elements but not for its eigenvalues. We cannot therefore make any a priori assumption on the form of their PDF, nor on the one of the quadrupolar parameters derived from them through Eq. (2). It is therefore preferable to represent the EFG, not by the five quadrupolar parameters but instead by five quantities depending linearly on the tensor elements. A natural choice is the five non-zero irreducible spherical tensor elements (the four other ones are null because of the zero trace and the symmetry of the EFG tensor)

$$V_2^m, m = 0, \pm1, \pm2$$

However, to facilitate the derivation of the joint PDF of the quadrupolar parameters, Czjzek proposes to use instead their real equivalents which evidently still preserve additivity

$$U_0 = V_2^0$$

$$U_1 = \frac{1}{\sqrt{2}}(V_2^1 + V_2^{-1})$$

$$U_2 = \frac{1}{i\sqrt{2}}(V_2^1 - V_2^{-1})$$

$$U_3 = \frac{1}{i\sqrt{2}}(V_2^2 - V_2^{-2})$$
$$U_4 = \frac{1}{\sqrt{2}}(V_2^2 + V_2^{-2}) \quad (9)$$

From the Central Limit Theorem, we then know that regardless of the actual PDF of the structural parameters, the joint PDF of the U_i's tends to a multivariate normal distribution for large numbers of independent random structural parameters.

The Czjzek model's second step: statistical isotropy.

Furthermore, electro-neutrality requires, through Laplace's equation, that their mean be zero. Also, statistical isotropy requires the EFG tensor elements to be independently and identically distributed. Again, this latter proposition holds only for the U_i's but not for the eigenvalues of the EFG or, a fortiori, for the quadrupolar parameters η and υ_Q.

In summary, assuming applicability of the CLT and statistical isotropy we get the PDF of the EFG tensor elements and of the U_is:

$$\begin{aligned} P(U_0,U_1,U_2,U_3,U_4) &= \prod_{i=0}^{4} P(U_i) = \prod_{i=0}^{4} \frac{1}{\sqrt{2\pi}\sigma} \exp\left(-\frac{U_i^2}{2\sigma^2}\right) \\ &= \frac{1}{(2\pi)^{5/2}\sigma^5} \exp\left(-\frac{\sum_{i=0}^{4} U_i^2}{2\sigma^2}\right) \\ &= \frac{1}{(2\pi)^{5/2}\sigma^5} \exp\left(-\frac{S}{2\sigma^2}\right) \end{aligned} \quad (10)$$

Consistently with our assumption of statistical isotropy, this PDF is invariant by rotation since S is the square of the modulus of the EFG. σ^2 relates thus to the second moment of the modulus. Within the context of NMR, we also note that S verifies

$$S = \sum_{i=x,y,z}\sum_{j=x,y,z} V_{ij}^2 = \sum_{i=0}^{4} U_i^2 = \frac{3}{2}V_{ZZ}^2\left(1+\frac{\eta^2}{3}\right) \sim C_{Q\eta}^2 \quad (11)$$

This means that to a proportionality constant, σ^2 must also relate to the variance of the NMR quadrupolar product.

A.2. The Czjzek model's third step: change of variables

The problem now reduces to a change of random variables to obtain the joint PDF of η and υ_Q from Eqs. (2) and (10). For this purpose, we use the functional determinant calculated by Czjzek

$$\left|\frac{\partial(U_0,U_1,U_2,U_3,U_4)}{\partial(\nu_Q,\eta,\alpha,\beta,\gamma)}\right| = 2\sin\beta V_{ZZ}^4 \eta\left(1-\frac{\eta^2}{9}\right) \quad (12)$$

Thus, in summary, from the general Eqs. (2), (9) and (12) in the one hand, and, on the other hand from Eq. (10) which assumes applicability of the CLT and statistical isotropy, Czjzek makes a change of random variables and derives the exact analytical form of the joint PDF of quadrupolar parameters:

$$p_Q(\nu_Q,\eta) = \frac{1}{\sqrt{2\pi}\sigma^5}\nu_Q^4\eta\left(1-\frac{\eta^2}{9}\right)\exp\left[-\frac{\nu_Q^2\left(1+\frac{\eta^2}{3}\right)}{2\sigma^2}\right] \quad (13)$$

The expression of the parameter σ, which as already stated relates to the second moment of the norm of the EFG, will depend on the original structural parameters PDF and thus of the particular model of disorder under consideration.

The marginal distribution of η does not depend on σ (and cannot since it is dimensionless while σ is not). This means that characterizing the distribution of the asymmetry, for example through its mean and variance, cannot carry any purpose other than to check the applicability of the Czjzek model. So, it is important to note that within the validity of the Czjzek model, regardless of the value of σ, the average υ_Q is zero and the average η is

$$\langle\eta\rangle = 2\sqrt{3} - \frac{3\sqrt{3}}{2}\ln(3) \approx 0.610 \quad (14)$$

This is not so far from the value of 0.5 sometimes proposed in the literature for amorphous materials [28,41].

Incidentally, one can also note that the marginal distribution of υ_Q does depend on σ, and in particular that its variance is directly proportional to σ^2:

$$\left\langle \nu_Q^2 \right\rangle - \langle \nu_Q \rangle^2 = \left\langle \nu_Q^2 \right\rangle = \left(7 - 3/2\sqrt{3}\right)\sigma^2 \approx 4.40\sigma^2 \quad (15)$$

References

[1] J.B. d'Espinose de Lacaillerie, F. Barberon, K.V. Romanenko, O.B. Lapina, L. Le Polles, R. Gautier, Z.H. Gan, Mo-95 magic angle spinning NMR at high field: improved measurements and structural analysis of the quadrupole interaction in monomolybdates and isopolymolybdates, J. Phys. Chem. B 109 (2005) 14033–14042.

[2] G. Czjzek, J. Fink, F. Gotz, H. Schmidt, J.M.D. Coey, J.P. Rebouillat, A. Lienard, Atomic coordination and the distribution of electric-field gradients in amorphous solids, Phys. Rev. B: Condens. Matter 23 (1981) 2513–2530.

[3] C. Legein, J.Y. Buzare, J. Emery, C. Jacoboni, Electron-paramagnetic-resonance determination of the local-field distribution acting on Cr3+ and Fe3+ in transition-metal fluoride glasses (Tmfg), J. Phys.: Condens. Matter 7 (1995) 3853–3862.

[4] C. Legein, J.Y. Buzare, B. Boulard, C. Jacoboni, Short-range order quantification in transition-metal fluoride glasses (Tmfg) through Epr-spectra simulation, J. Phys.: Condens. Matter 7 (1995) 4829–4846.

[5] J. Kliava, R. Berger, Y. Servant, J. Emery, J.M. Greneche, J. Trokss, Electron paramagnetic resonance and Mossbauer effect studies in iron-doped Fe-57 isotope enriched phosphate glasses, J. Non-Cryst. Solids 202 (1996) 205–214.

[6] C. Legein, J.Y. Buzare, C. Jacoboni, The local field distribution of Gd3+ in transition metal fluoride glasses investigated by electron paramagnetic resonance, J. Phys.: Condens. Matter 8 (1996) 4339–4350.

[7] L.C. Damonte, L.A. Mendoza-Zelis, S. Deledda, J. Eckert, Effect of preparation conditions on the short-range order in Zr-based bulk glass-forming alloys, Mater. Sci. Eng. A 343 (2003) 194–198.

[8] J.M. Greneche, Local structural order in disordered systems investigated by Mossbauer spectrometry, J. Non-Cryst. Solids 287 (2001) 37–44.

[9] B. Bureau, G. Silly, J.Y. Buzare, C. Legein, D. Massiot, From crystalline to glassy gallium fluoride materials: an NMR study of 69Ga and 71Ga quadrupolar nuclei, Solid State Nucl. Magn. Reson. 14 (1999) 181–190.

[10] B. Bureau, G. Silly, J.Y. Buzare, B. Boulard, C. Legein, Nuclear magnetic resonance quadrupolar parameters and short range order in disordered ionic fluorides, J. Phys.: Condens. Matter 12 (2000) 5775–5788.

[11] D.R. Neuville, L. Cormier, D. Massiot, Al environment in tectosilicate and peraluminous glasses: a 27Al MQ-MAS NMR, Raman, and XANES investigation, Geochim. Cosmochim. Acta 68 (2004) 5071–5079.

[12] F. Angeli, M. Gaillard, P. Jollivet, T. Charpentier, Contribution of 43Ca MAS NMR for probing the structural configuration of calcium in glass, Chem. Phys. Lett. 440 (2007) 324–328.

[13] C.O. Arean, M.R. Delgado, V. Montouillout, D. Massiot, Synthesis and characterization of spinel-type gallia–alumina solid solutions, Z. Anorg. Allg. Chem. 631 (2005) 2121–2126.

[14] D. Massiot, F. Fayon, M. Capron, I. King, S. Le Calve, B. Alonso, J.O. Durand, B. Bujoli, Z.H. Gan, G. Hoatson, Modelling one- and two-dimensional solid-state NMR spectra, Magn. Reson. Chem. 40 (2002) 70–76.

[15] G.M. Bowers, K.T. Mueller, Electric field gradient distributions about strontium nuclei in cubic and octahedrally symmetric crystal systems, Phys. Rev. B: Condens. Matter 71 (2005) 224112–224117.

[16] T.M. Clark, P.J. Grandinetti, Calculation of bridging oxygen quadrupolar coupling parameters in alkali silicates: a combined ab initio investigation, Solid State Nucl. Magn. Reson. 27 (2005) 233–241.

[17] S. Nagel, Cluster calculation of electronic structure and quadrupole interaction in alpha-Al2O3, J. Phys. C: Solid State Phys. 18 (1985) 3673–3685.

[18] B. Winkler, P. Blaha, K. Schwarz, Ab initio calculation of electric-field-gradient tensors of forsterite, Am. Mineral. 81 (1996) 545–549.

[19] P. Losso, U. Sternberg, Distribution of principal values of the 31P NMR chemical shift tensor in phosphate glasses, Solid State Nucl. Magn. Reson. 13 (1998) 113–118.

[20] J.R. Sachleben, Bayesian and information theory analysis of MAS sideband patterns in spin 1/2 systems, J. Magn. Reson. 183 (2006) 123–133.

[21] D. Massiot, A. Kahn-Harari, D. Michel, D. Muller, F. Taulelle, Aluminium-27 MAS NMR of Al_2G2O_7 and $LaAlGe_2O_7$: two pentacoordinated aluminium environments, Magn. Reson. Chem. 28 (1990) S82–S88.

[22] D.T. Gillespie, A theorem for physicists in the theory of random variables, Am. J. Phys. 51 (1983) 520–533.

[23] T. Charpentier, S. Ispas, M. Profeta, F. Mauri, C.J. Pickard, First-principles calculation of ^{17}O, ^{29}Si, and ^{23}Na NMR spectra of sodium silicate crystals and glasses, J. Phys. Chem. B 108 (2004) 4147–4161.

[24] G. Kunath-Fandrei, T.J. Bastow, J.S. Hall, C. Jaeger, M.E. Smith, Quantification of aluminum coordinations in amorphous aluminas by combined central and

satellite transition magic angle spinning NMR spectroscopy, J. Phys. Chem. 99 (1995) 15138–15141.
[25] W. Storek, R. Muller, G. Kunath-Fandrei, 27Al and 29Si MAS NMR investigations of cordierite glass, [mu]- and [alpha]-cordierite, Solid State Nucl. Magn. Reson. 9 (1997) 227–239.
[26] R.H. Meinhold, R.C.T. Slade, R.H. Newman, High-field Mas Nmr, with simulations of the effects of disorder on lineshape, applied to thermal transformations of alumina hydrates, Appl. Magn. Reson. 4 (1993) 121–140.
[27] D. Coster, A.L. Blumenfeld, J.J. Fripiat, Lewis-acid sites and surface aluminum in aluminas and zeolites - a high-resolution Nmr-study, J. Phys. Chem. 98 (1994) 6201–6211.
[28] G.L. Hoatson, D.H.H. Zhou, F. Fayon, D. Massiot, R.L. Vold, Nb-93 magic angle spinning NMR study of perovskite relaxor ferroelectrics (1-x)Pb(Mg1/3Nb2/3)O-3-xPb(Sc1/2Nb1/2)O-3, Phys. Rev. B: Condens. Matter 66 (2002) 224103.
[29] P. Jeglic, M. Komelj, M. Klanjsek, U. Tkalec, S. Vrtnik, M. Feuerbacher, J. Dolinsek, Orientation-dependent NMR study of the giant-unit-cell intermetallics beta-Al_3Mg_2, Bergman-phase $Mg_{32}(Al,Zn)_{49}$, and xi-$Al_{74}Pd_{22}Mn_4$, Phys. Rev. B: Condens. Matter 75 (2007) 014202–014215.
[30] D.R. Neuville, L. Cormier, D. Massiot, Al coordination and speciation in calcium aluminosilicate glasses: effects of composition determined by 27Al MQ-MAS NMR and Raman spectroscopy, Chem. Geol. 229 (2006) 173–185.
[31] C.O. Areán, M.R. Delgado, V. Montouillout, D. Massiot, Synthesis and characterization of spinel-type gallia–alumina solid solutions, Z. Anorg. Allg. Chem. 631 (2005) 2121–2126.
[32] M.R. Hill, T.J. Bastow, S. Celotto, A.J. Hill, Integrated study of the calcination cycle from gibbsite to corundum, Chem. Mater. 19 (2007) 2877–2883.
[33] G. Gutiérrez, B. Johansson, Molecular dynamics study of structural properties of amorphous Al_2O_3, Phys. Rev. B 65 (2002) 104202.
[34] G. Gutiérrez, A. Taga, B. Johansson, Theoretical structure determination of gamma-Al_2O_3, Phys. Rev. B 65 (2001) 012101.
[35] K.L. Scrivener, T. Fullmann, E. Gallucci, G. Walenta, E. Bermejo, Quantitative study of Portland cement hydration by X-ray diffraction/Rietveld analysis and independent methods, Cement Concrete Res. 34 (2004) 1541–1547.
[36] M.R. Hartman, R. Berliner, Investigation of the structure of Ettringite by time-of-flight neutron powder diffraction techniques, Cement Concrete Res. 36 (2006) 364–370.
[37] M.D. Andersen, H.J. Jakobsen, J. Skibsted, A new aluminium-hydrate species in hydrated Portland cements characterized by 27Al and 29Si MAS NMR spectroscopy, Cement Concrete Res. 36 (2006) 3–17.
[38] G. Le Caër, R.A. Brand, General models for the distributions of electric field gradients in disordered solids, J. Phys.: Condens. Matter 10 (1998) 10715–10774.
[39] A. Samoson, Satellite transition high-resolution NMR of quadrupolar nuclei in powders, Chem. Phys. Lett. 119 (1985) 29–32.
[40] P. Florian, N. Sadiki, D. Massiot, J.P. Coutures, 27Al NMR study of the structure of lanthanum- and yttrium-based aluminosilicate glasses and melts, J. Phys. Chem. B 111 (2007) 9747–9757.
[41] L. Zhang, H. Eckert, Short- and medium-range order in sodium aluminophosphate glasses: new insights from high-resolution dipolar solid-state NMR spectroscopy, J. Phys. Chem. B 110 (2006) 8946–8958.